SYNTHESIS AND CHARACTERIZATION OF Co-Zn FERRITE NANOCRYSTALS FOR MAGNETOCALORIC APPLICATIONS

S. Urcia-Romero[1], B. Renteria[2], O. Perales-Pérez[2] and G. Gutiérrez[3]
[1] University of Puerto Rico, Department of Physics P.O. Box 9016, Mayagüez, P.R. 00681-9016
[2] University of Puerto Rico, Department of Engineering Science & Materials P.O. Box 9044, Mayagüez, P.R. 00680-9044
[3] University of Puerto Rico, Department of Mechanical Engineering, P.O. Box 9045, Mayagüez, P.R. 00681-9045

ABSTRACT

Cobalt-Zinc ferrite is known for its chemical stability and composition-sensitive demagnetization temperature. In this work, $Co_xZn_{1-x}Fe_2O_4$ nanocrystals have been synthesized by conventional and size-controlled co-precipitation methods. The effect of Co^{2+} atomic fraction, 'x', on the magnetic properties of nanocrystals was investigated. The average crystallite size of the ferrite nanocrystals synthesized by conventional co-precipitation ranged between 8.8 nm and 13.6 nm for 'x' between 0.5 and 1.0, respectively. The corresponding maximum magnetization varied from 24emu/g to 60emu/g. The coercivity value was increased by a rising 'x' or by producing the nanocrystals under size-controlled synthesis conditions. This increase in coercivity was attributed to both, an increase in the magnetic anisotropy energy and the promotion of crystal growth within the single domain region. As expected, the demagnetization temperature was strongly dependent on the ferrite composition.

Keywords: Co-Zn ferrite, nanocrystals, Magnetocaloric applications, demagnetization temperature.

INTRODUCTION

The synthesis of nanocrystals is currently an intensive research area due to the verified size-dependence of their functional properties and wide range of applications [1]. Magnetic fluids, a suspension of ferromagnetic nanoparticles in suitable solvents, find novel applications in areas such as diagnostic biomedicine, drug delivery, or genetic sequencing. Nethe et al. used a novel motor driven by a ferrofluid for a ventricular assist device [2, 3], as well as for cell separation [4]. These ferrites also find application in galvanometers, inclinometers, voice coil actuators, stepper motors, etc [5, 6].

Rosensweig has proposed a possibility to pump a magnetic fluid by using their magnetic and thermal properties [7]. In the presence of a uniform and constant magnetic field, the entropy associated with the magnetic degree of freedom in the magnetic particles changes due to ordering of the magnetic moments in the direction of the applied field. A pressure gradient can be set up if there is an increase in temperature. If the temperature of the ferrofluid increases and approaches its demagnetization temperature (T_C), it loses its magnetization and can be replaced by a volume of cooler fluid. This phenomenon allows propulsion of the magnetic fluid without the necessity of moving parts, thereby reducing or eliminating mechanical wear and extending the lifetime of the device [8]. The optimal material for this kind of application should have a demagnetization temperature close to the maximum operating temperature of the system as well as a high magnetization and thermomagnetic coefficient (dM/dT) to maximize the pressure gradient.

Cobalt ferrite ($CoFe_2O_4$) is known for its high coercivity and chemical stability. The T_C temperature of this material becomes composition-sensitive when Cobalt is partially substituted by Zinc species. Accordingly, a magnetic fluid bearing this type of ferrite nanocrystals could be then considered a candidate for magnetocaloric energy conversion application [1, 9]. In the present work, we investigate the influence of the composition and crystal size of cobalt-zinc ferrite nanocrystals ($Co_xZn_{1-x}Fe_2O_4$) on their magnetic properties. The nanocrystals were synthesized by conventional and size-controlled coprecipitation approaches. In the later, the nanoparticles were formed by control of the oversaturation conditions in reacting solution.

1 EXPERIMENTAL

1.1 Materials

Required weights of the chloride salts of Fe, Zn, and Co ions were dissolved in distilled water to achieve the desired Fe/Me mole ratio of two (Me = Co^{+2} + Zn^{+2}) according to $Co_xZn_{1-x}Fe_2O_4$ stoichiometry. NaOH in aqueous solution was used as the alkaline precipitant. All reagents were used without further purification.

1.2 Synthesis of Ferrite Nanocrystals

Ferrite nanocrystals were synthesized by the conventional and modified co-precipitation methods. In the conventional method, an aqueous solution of 0.055 mol Co(II) + Zn(II) together with 0.11 mol Fe(III) were added to an aqueous solution of 0.48 mol NaOH that was kept boiling and under mechanical stirring at 500 rpm. After the precursor salts were added, the solution was kept boiling for one hour to allow for a complete dehydration and atomic rearrangement involved with the formation of ferrite particles.

The conventional co-precipitation method was modified to control the oversaturation conditions during the ferrite formation in aqueous phase. This control was achieved by

the precise control of the flow-rate at which the metal-salt precursors were added to the hydroxide solution. For this purpose, a micro-peristaltic pump was utilized. At the end of the reaction time, the nanoparticles were washed with deionized water and dried at 80 °C for 24 hours.

1.3 Characterization Techniques

Structural characterization of the solids were carried out in a Siemens D500 x-ray diffractometer (XRD) using the Cu-Kα radiation. The average crystallite size of the produced powders was estimated by using Scherrer's equation for the peaks identified. Magnetic measurements on the powdered samples were performed in a LakeShore vibrating sample magnetometer unit (VSM). Magnetization vs. applied field, MH, measurements were performed at room temperature in fields up to 2.2 tesla, while magnetization-temperature, MT, measurements were performed under 0.5 Tesla in the temperature range between 30 °C and 600 °C. Measured parameters include maximum magnetization, remnant magnetization, and coercive field as function of the atomic fraction of Co, 'x', and flow rate of the addition of reactants.

2 RESULTS AND DISCUSSION

2.1 XRD Analyses

XRD analyses confirmed the formation of the ferrite structure at all composition levels (Fig. 1). When the synthesis took place with no control of the flow-rate of the addition of reactants, the average crystallite size was strongly dependent on the atomic fraction of Co species, 'x'. It varied from 8.8 nm to 13.6 nm when 'x' was increased from 0.5 to 1.0.

'x'	D (nm) +/-0.3	a (Å) +/-0.3
0.5	8.8	8.313
0.6	11.0	8.331
0.8	11.33	8.339
0.9	12.39	8.340
1.0	13.59	8.345

Table 1. Variation in average crystallite size, 'D', and lattice parameter, 'a', with the atomic fraction of Co ions, 'x'. The nanoparticles were synthesized with no control of flow-rate.

The larger fractions of Zn species, i.e. lower 'x' values, would have affected the solubility of the combined hydroxide precursor and hence, the ferrite nucleation rate. As suggested by the values shown in Table 1, the lattice parameter did not exhibit a drastic variation in the evaluated 'x' range. The similitude between the ionic radiuses of Co^{2+} (0.072 nm) and Zn^{2+} (0.074 nm) ions can explain this negligible variation. The size-controlled synthesis of Co-Zn ferrite nanocrystals was evaluated for 'x' = 0.5, 0.8, and 0.9 and flow-rates of 1 mL/min, 5 mL/min, and 20 mL/min. The most remarkable effect of the variation in flow-rate was on the average crystallite size of the particles. For instance, the average crystallite size varied from 11.3 nm (no control of flow-rate) to 17.7 nm when the nanoparticles were synthesized at 1mL/min and 'x' = 0.8. Similar trends were observed for the other 'x' values. In general, the average crystallite size decreased by a rising flow-rate (Figure 2).

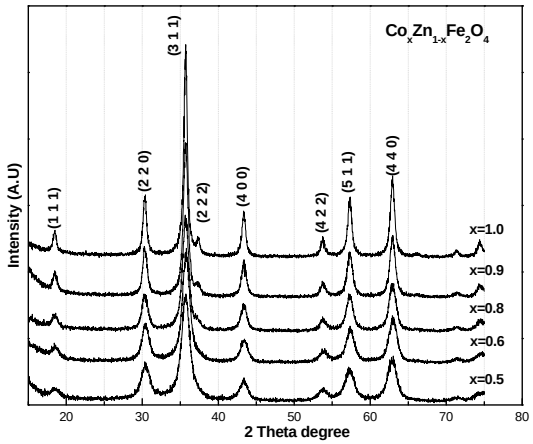

Fig 1. XRD patterns for CoZn ferrite powders synthesized at various atomic fractions of Co ions, 'x'.

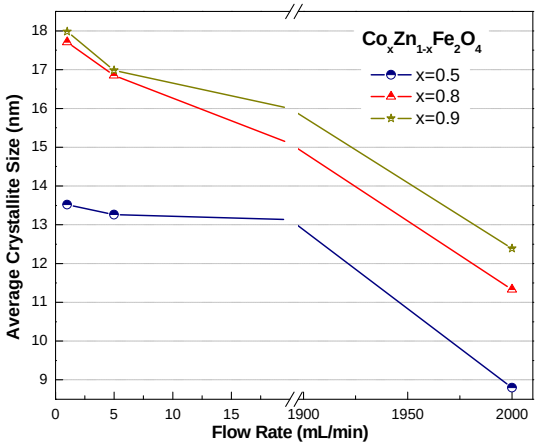

Fig 2. Variation of average crystallite size with flow-rate at different atomic fractions of Co ions, 'x'.

'x'	D (nm) +/-0.3			a (Å) +/-0.3		
	1 mL/min	5 mL/min	20 mL/min	1 mL/min	5 mL/min	20 mL/min
0.5	13.5	13.3	13.3	8.369	8.369	8.360
0.8	17.7	16.9	15.1	8.395	8.395	8.360
0.9	18.0	17.0	16.0	8.367	8.353	8.360

Table 2. Lattice parameter, 'a', and crystallite size, 'D', of Co-Zn ferrite nanoparticles synthesized at different flow rates and 'x' values.

NSTI-Nanotech 2009, www.nsti.org, ISBN 978-1-4398-1782-7 Vol. 1, 2009

The objective of controlling the flow-rate was to achieve the best possible conditions for heterogeneous nucleation where early formed nuclei should have acted as seeds and promoted further crystal growth.

2.2 M-H Measurements

Figure 3 shows the M-H curves for $Co_xZn_{1-x}Fe_2O_4$ nanocrystals synthesized by the conventional co-precipitation method. It can be seen that the maximum magnetization increases with the atomic fraction of Co species. The incorporation of magnetic Co^{2+}-cations replacing the non-magnetic Zn^{2+} explains the enhancement in the maximum magnetization with a rising 'x'. Furthermore, the coercivity of the samples was also increased by increasing the contents of Co. This trend in coercivity can be attributed to the ferrite composition and the distribution of metal ions in specific lattice sites in the ferrite structure. For this mixed ferrite structure the magnetic ordering is determined by super-exchange interactions between metal ions on the lattice A- and B-sites. The Fe^{3+}-ions in cobalt-free $ZnFe_2O_4$ occupy the octahedral B-sites and half of the tetrahedral A-sites with the other half of A-sites occupied by Zn^{2+} species. However, the divalent Co^{2+} and Zn^{2+} species in $Co_xZn_{1-x}Fe_2O_4$ structure are expected to occupy the octahedral B-sites whereas only Fe^{3+} species would be located in the tetrahedral A-sites [10].

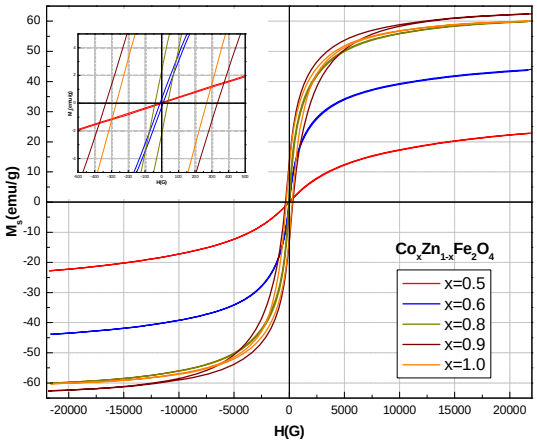

Fig 3. M-H loops of Co-Zn ferrite synthesized with no control of flow-rate and various Co atomic fractions, 'x'. The inset shows the M-H data at the origin.

Regarding the magnetic properties of those samples synthesized under flow-controlled conditions, the most noticeable effect was the remarkable enhancement on coercivity. For 'x' = 0.8 the coercivity increased from 38 G (no control of flow-rate) to 706 G when the flow-rate was 1 mL/min. The variation in coercivity was even more drastic for 'x' = 0.9; it was increased from 334 G (no-control) to 1,683 G at the same flow-rate. In absence of a more detailed evaluation of any probable atomic rearrangement promoted by synthesis conditions, this rise in coercivity can be attributed to the enlargement of the crystallite size, which was suggested by XRD measurements.

'x'	M_{max} (emu/g)				H_C (G)			
	1 mL/min	5 mL/min	20 mL/min	No control	1 mL/min	5 mL/min	20 mL/min	No control
0.5	28	31	31	24	18	15	23	8
0.8	46	56	59	60	706	259	290	38
0.9	51	56	62	63	1683	510	934	334

Table 3. Maximum magnetization 'M_{max}' and coercivity 'H_C' for Co-Zn ferrite synthesized at different 'x' values with and with no control of flow-rate.

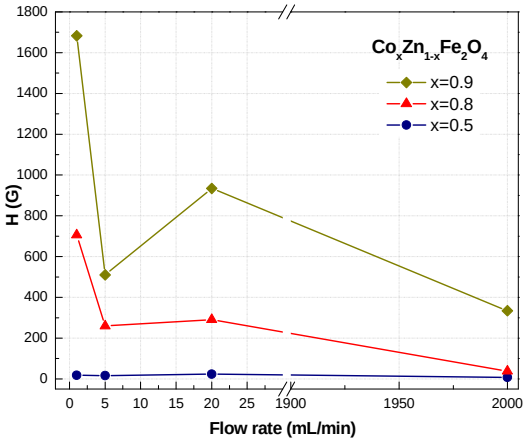

Fig 4. Variation of coercivity with flow rate for 'x' = 0.5, 0.8 and 0.9.

2.3 M-T Measurements

M-T measurements were carried out for samples produced at 'x' = 0.5, 0.8 and 0.9, with (1 mL/min) and without control of the flow-rate (Figures 5 and 6, respectively). The corresponding results are summarized in Table 4. The demagnetization temperature, T_C, was estimated by extrapolating the linear part of the M-T curve when the magnetization approaches to zero. The non-linear portion in the M-T plot is consequence of the redistribution of Zn-, Co-, and Fe-ions in the tetrahedral A-sites and octahedral B-sites at high temperatures [11]. The data in Table 4 also indicates that the higher the atomic fraction of Co species, the higher the T_C. This dependence of T_C with composition of the material has also been observed in Mn-Zn and Ni-Zn ferrites and was explained in terms of the replacement of the magnetic ions from the tetrahedral A-site with non-magnetic Zn ions in the ferrite structure. It will result in the reduction of the exchange interaction between the magnetic ions with Fe in the ferrite octahedral B-sites and, consequently, the decrease in the demagnetization temperature [9, 11, 12]. A minor, but noticeable, decrease of T_C when the nanocrystals ('x'= 0.8 and 0.9) were synthesized with control of low-rate became also evident. Interestingly, T_C was clearly increased from

120°C to 170°C when the powders were synthesized at 'x' 0.5 and 1mL/min. The reasons behind this variation are still under investigation.

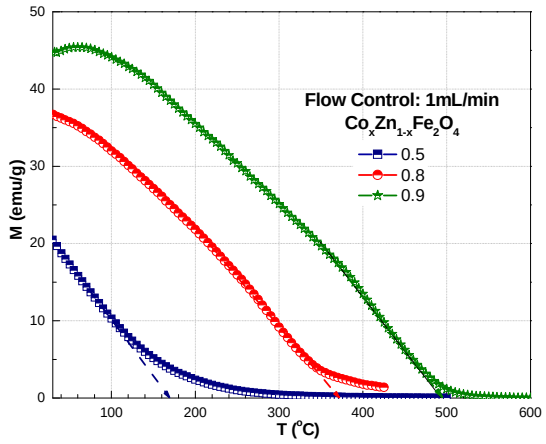

Fig 5. M-T profiles for Co-Zn ferrites synthesized at 1 mL/min and various 'x' values. The external magnetic field was 0.5T.

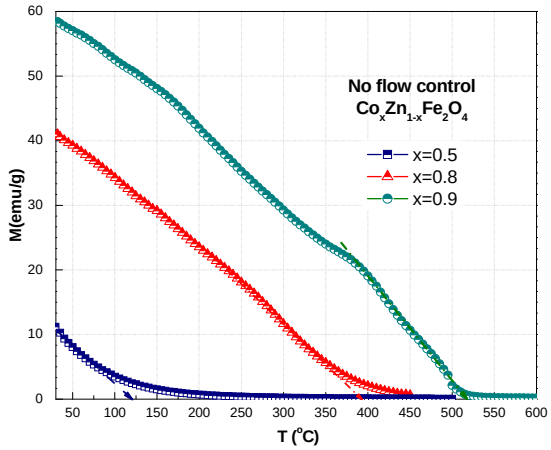

Fig 6. M-T profiles for Co-Zn ferrite synthesized without control of flow-rate (conventional co-precipitation) and various 'x' values. The external magnetic field was 0.5T.

'x'	T_C (°C)	
	1mL/min	No control
0.5	170	120
0.8	368	390
0.9	490	515

Table 4. Demagnetization temperature, T_C, of ferrite nanocrystals synthesized at various 'x' values with (1 mL/min) and without control of low-rate.

The pyromagnetic coefficient (K_T) was calculated, from the slope of the linear portion in MT plots. The K_T values did not change with the synthesis method and ranged between 0.19 emu/g-K and 0.17 emu/g-K when 'x' varied from 0.5 to 0.9, respectively. Ongoing work is focused on the study of the magnetic structure in these ferrites by Mossbauer spectroscopy.

3 CONCLUDING REMARKS

We have demonstrated the viability on controlling crystal size and the subsequent effect on the magnetic properties of Co-Zn ferrite nanocrystals. The nanoparticle average crystallite size increases by increasing Co-concentration or lowering the flow-rate at which the reactants are contacted. For a given Co-concentration, the coercivity increases up to a factor of five under flow-rate controlled synthesis condition, while the maximum magnetization turns out to be much less affected. The Tc values of the Co-Zn ferrite powders decreased at lower atomic fractions of Co species. A minor, but noticeable, decrease in the Tc was also observed when the synthesis was carried out at 1mL/min for 'x' 0.8 or 0.9.

4 ACKNOWLEDGMENTS

This material is based upon work supported by the US-Department of Defense under Award 50797 – RT-ISP.

REFERENCES

[1] E. Avzans D. Zins, E. Blums, and R. Massart, J. Mater. Sci. 34, 1999.
[2] L. Love, J. Jansen, T. Mcknight, Y. Roh and T. Phelps, IEEE Transaction on Nanobiosciencie , Vol. 3, No. 2, June 2004.
[3] A. Nethe, T. Schoppe, and H. Stahlmann, J. Magn. Magn. Mater., Vol. 201, pp.423–426, 1999.
[4] B. Martin, Pren. Diagn., Vol. 17, no. 11, pp.1059–1066, 1997.
[5] K. Raj, B. Moskowitz, and R. Casciari J. Magn. Magn. Mater. Vol. 149, pp. 174–180, 1995.
[6] L. Cao and H. Schwartz, Nonlin. Dyn., Vol. 180, no. 4, pp. 383–404, 1999.
[7] R. Rosensweig, Ferrohydrodynamics. Mineola, NY: Dover, 1985.
[8] B. Ando, A. Ascia, S. Baglio, N. Pitrone – Annual International Conference, NY City, August-30, 2006.
[9] G.Vaidyanathan, Sendhilnathan, R Arulmurugan J. Magn. Magn. Mater., 313, 293 – 299, 2007.
[10] B. Cushing, V. Koleesnichenco and C. O'Connor – Chem. Rev., 104, 3893-3946, 2004.
[11] C. Rath, S. Anand, R. Das, K. Sahu, S. Kulkarni, S. Date and N. Mishra, J. Appl. Phys. 91, 2211, 2002.
[12] R.V. Upadhyay, R.V. Mehta, Kinnari Parekh, D. Sriniva, R.P. Pant, J. Magn. Magn. Mater., vol. 201, pp. 129-132, 1999.